

comes

$$E_q = [A_q^2 - (|B_q| \pm |D_q|)^2]^{1/2}.$$

Here A_q and D_q are just the first and second parts of our Eq. (6), and B_q is an intrasublattice anisotropic exchange term of the form

$$J^{xx}(q) - J^{yy}(q) + i[J^{xy}(q) + J^{yx}(q)].$$

Since $|D_q|$ is very small, it is clear that $|B_q|$ would have to be anomalously large in order to produce an observable splitting.

²⁸T. Riste, Nucl. Instr. Methods **86**, 1 (1970); A. C. Nunes and G. Shirane, *ibid.* **95**, 445 (1971).

²⁹G. Shirane and V. J. Minkiewicz, Nucl. Instr. Methods **89**, 109 (1970).

³⁰C. Zener, Phys. Rev. **96**, 1335 (1954); J. Kanamori and M. Tachiki, J. Phys. Soc. Japan **17**, 1384 (1962); H. B. Callen and E. Callen, J. Phys. Chem. Solids **27**, 1271 (1966).

³¹T. Tonegawa, Progr. Theoret. Phys. (Kyoto) Suppl. **46**, 61 (1970).

³²F. J. Dyson, Phys. Rev. **102**, 1217 (1956); **102**, 1230 (1956).

³³R. J. Birgeneau, J. Skalyo, Jr., and G. Shirane, Phys. Rev. B **3**, 1736 (1971).

³⁴S. Hautecler, J. Konstatinovic, D. Cribier, and B. Jacrot, Compt. Rend. **254**, 1026 (1962).

Magnetic Properties of FeCl₂ in Zero Field. II. Long-Range Order

W. B. Yelon

Brookhaven National Laboratory, * Upton, New York 11973

and

R. J. Birgeneau[†]

Bell Laboratories, Murray Hill, New Jersey 07974

(Received 15 September 1971)

In Paper I it has been shown that the critical behavior of FeCl₂ in zero field should be that appropriate to the three-dimensional $S=1$ Ising model. This paper reports a detailed study of the critical behavior of the sublattice magnetization below T_N together with a qualitative survey of the wave-vector-dependent susceptibility above T_N . The sublattice magnetization is found to follow the power law $M_T/M_0 = D(1 - T/T_N)^\beta$, with $D = 1.47 \pm 0.02$, $T_N = 23.553 \pm 0.01$ °K, $\beta = 0.29 \pm 0.01$, over the range 0.1 to <0.001 in reduced temperature. The exponent β is in reasonable agreement with the rigid-lattice Ising value of 0.313 ± 0.003 . The regular behavior of M_T together with the unusual metamagnetic properties of FeCl₂ make this an ideal system for a study of the critical behavior of the order parameter around a tricritical point. The wave-vector-dependent susceptibility $\chi^{\alpha\alpha}(\vec{Q})$ above T_N is found to exhibit typical behavior for a three-dimensional anisotropic antiferromagnet. Only $\chi^{\alpha\alpha}(\vec{\tau})$, the component along the anisotropy axis, diverges at the phase transition. Furthermore $\chi^{\alpha\alpha}(\vec{Q})$ is found to be fully three dimensional; that is, it has the form of a peak rather than a ridge, in spite of the fact that the spin waves are essentially two dimensional in form.

I. INTRODUCTION

The critical properties of FeCl₂ in zero field are of interest for two principal reasons. As we have seen in the previous paper, the spin waves have a pronounced two-dimensional character with the inter- and intraplanar interactions differing by about a factor of 20. FeCl₂ thus lies intermediate between such antiferromagnets as KNiF₃, which is fully three dimensional and ¹K₂NiF₄, which exhibits a "two-dimensional" phase transition. The behavior of both the order parameter in the antiferromagnetic regime and the correlations in the paramagnetic phase in such an intermediate-dimensional compound should be quite interesting. In par-

ticular, one anticipates that the critical behavior will be fully three dimensional in spite of the directional nature of the interactions.²

A second motivation for studying the critical behavior of FeCl₂ in zero field is, of course, to evaluate the suitability of FeCl₂ for detailed tricritical-point studies.³ The critical behavior may be affected both by Fe³⁺ contamination and by spin-phonon effects. The latter could be particularly important in this case because of the extreme softness of the lattice and the large orbital contribution to the effective $S=1$ moment. Such effects could manifest themselves either through a smearing of the phase transition or renormalization of the critical exponents.

The order parameter in an antiferromagnet is simply the sublattice magnetization M_T . In the asymptotic limit the sublattice magnetization should exhibit a power-law dependence² on the reduced temperature

$$M_T/M_0 = D(1 - T/T_N)^\beta. \quad (1)$$

In the previous paper,⁴ it was shown that the low-lying states in FeCl_2 could be adequately described by an effective-spin $S=1$ Hamiltonian with Heisenberg exchange and a strong uniaxial-anisotropy field. The latter originates both from the crystal field and from bilinear-anisotropic-exchange terms in the effective-spin Hamiltonian. As first shown by Jasnow and Wortis,⁵ the asymptotic critical behavior of such a system should depend on the symmetry of the Hamiltonian alone and not on its details. Thus the critical behavior of FeCl_2 should be that appropriate to a three-dimensional $S=1$ Ising model.

Recently, series-expansion calculations have been reported by Guttman *et al.* and Fox *et al.*⁶ for the $S=1$ Ising model on various cubic lattices. They find

$$\beta = 0.313 \pm 0.003, \quad (2)$$

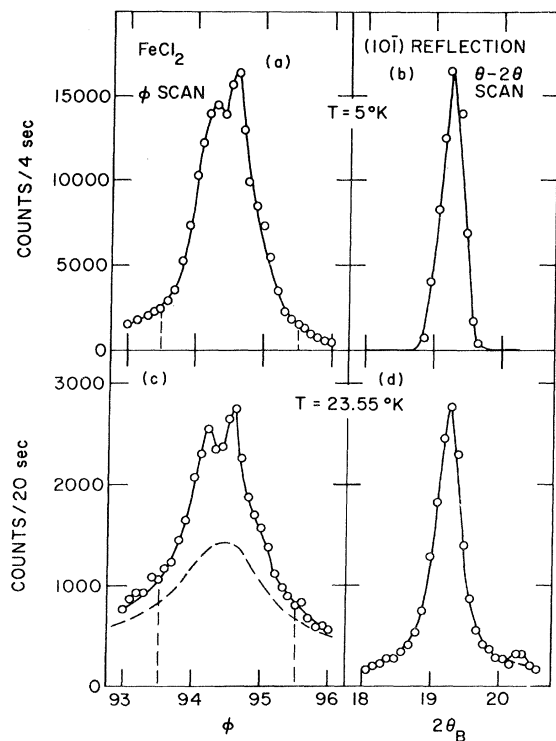


FIG. 1. Typical ϕ and $\theta-2\theta$ scans through the $(1, 0, \bar{1})$ superlattice reflection in FeCl_2 below T_N . As is evident from part (a), the mosaic is both double peaked and distinctly non-Gaussian. The dotted line in (c) is the estimated critical-scattering contribution.

in agreement with the $S=\frac{1}{2}$ value,^{7,8} as expected on general grounds. The coefficient D has also been evaluated; unlike β , D is both spin and lattice dependent. Since calculations for the actual FeCl_2 structure are not available, we can only use the cubic-lattice values as a qualitative guide.

In this paper we report a detailed study of the sublattice magnetization of FeCl_2 in zero field together with a qualitative survey of the wave-vector-dependent susceptibility $\chi^{\alpha\alpha}(\vec{Q})$ above T_N . The experimental methods are discussed in Sec. II. Sections III and IV report, respectively, the results and the analysis of the order-parameter measurements. In Sec. V, the theory of $\chi^{\alpha\alpha}(\vec{Q})$ in the molecular-field approximation together with the experimental results are presented. Finally, the conclusions are given in Sec. VI.

II. EXPERIMENTAL PROCEDURE

The sublattice magnetization was measured by observing the intensity of magnetic-superlattice Bragg peaks with a double-axis neutron spectrometer. The (311) reflection from a germanium monochromator was used, providing an incoming neutron beam with 1.03-\AA wavelength. This reflection minimized contamination from $\frac{1}{2}\lambda$ neutrons, and measurements above T_N showed that this contamination as well as double Bragg scattering was almost negligible.

Since the sample mosaic was quite large ($\sim 1^\circ$) and the sample possibly nonhomogeneous due to Fe^{3+} impurities, it was not obvious that the Néel point was uniform. However, the irregular mosaic shape [see Fig. 1(a)] enabled us essentially to monitor the temperature dependence of distinct parts of the crystal; the constancy of that shape, even very close to T_N , was convincing evidence that the spread in T_N and also any temperature gradient across the sample were less than 10 mdeg K. The temperature of the heat sink could be held constant near the Néel point (23.55_3°K) to at least ± 10 mdeg K. The sample was attached by epoxy to the heat sink some distance from the thermometer so that it was difficult to estimate the absolute temperature at the sample to better than 100 mdeg K, although relative changes were known rather more accurately. After each temperature change, adequate time was taken for the sample to reach thermal equilibrium. This time was empirically defined by observing the magnetic Bragg peak and measurements were not begun until the intensity of that peak remained constant for several minutes. This, of course, became an increasingly stringent criterion as the Néel temperature was approached since dI/dT increased as $T_N - T$ decreased.

Allowance must be made for several important effects when measuring the intensities of the superlattice points. There is, first, a temperature-in-

dependent background, resulting from $\frac{1}{2}\lambda$, double Bragg, and incoherent scattering. The strength and angular dependence of this may be determined by scanning at a temperature above T_N such that critical magnetic scattering is not appreciable, but at a temperature that is still relatively low. This background can then be subtracted from the Bragg peak to give the correct magnetic portion. Extinction of strong peaks may be a more difficult effect to correct for. However, such effects are usually noticeable only in relatively perfect crystals; the large mosaic of our sample suggests that the extinction should be small. It was possible to check for extinction by examining the temperature dependence

TABLE I. Intensities and corrections for the (1 0 $\bar{1}$) and (2 0 1) magnetic reflections. The counting time was doubled above 22.25 °K and multiplied by five above 23.475 °K. The error quoted is consistently larger than the statistical error, and is estimated to include other experimental uncertainties such as temperature control.

Peak	T (°K)	Intensity background unit time	I (critical scattering)	$\frac{M_T}{M_0}$ M_0 °K	Error (%)
(1 0 $\bar{1}$)	5.0	172 273		1.000	
	9.0	167 047		0.988	0.25
	13.0	162 539		0.971	0.25
	16.0	150 004		0.933	0.25
	18.0	136 621		0.891	0.25
	19.0	125 391		0.853	0.25
	20.0	114 417		0.815	0.25
	21.0	100 676		0.764	0.5
	21.5	90 474		0.725	0.5
	21.75	84 481		0.700	0.5
	22.0	78 045		0.673	0.5
	22.25	71 207		0.643	0.5
	22.50	64 143		0.610	0.5
	22.75	54 201		0.561	0.5
	23.00	43 593		0.503	0.5
	23.10	38 317		0.472	0.5
	23.20	33 650		0.442	0.5
	23.30	27 930		0.403	0.5
	23.35	25 501		0.385	0.5
	23.40	20 668		0.346	0.5
	23.44	17 264	100	0.317	0.5
	23.475	14 561	350	0.287	0.5
	23.500	11 969	504	0.255	1.0
23.525	8 441	840	0.210	1.0	
23.550	6 208	3 624	0.122	2.0	
(2 0 1)	5.0	24 577		1.000	1.0
	9.0	24 131		0.991	1.0
	13.0	22 791		0.963	1.0
	16.0	21 351		0.932	1.0
	18.0	19 455		0.890	1.0
	19.0	18 232		0.861	1.0
	20.0	16 424		0.817	1.0
	21.0	14 336		0.764	1.0
	21.50	12 736		0.720	1.0
	21.75	11 962		0.698	1.0
	22.00	11 064		0.671	1.0
	22.25	9 873		0.634	1.25
	22.50	8 977		0.604	1.0
	22.75	7 761		0.562	1.0
	23.00	6 209		0.503	1.0
	23.10	5 565		0.476	1.0
	23.20	4 882		0.446	1.5
23.30	4 029		0.405	1.5	
23.40	3 106		0.355	2.0	

of the intensity ratio of two different-strength magnetic Bragg peaks. The (1 0 $\bar{1}$) and the (2 0 1) reflections differed in intensity by about a factor of 7 due to the magnetic form factor at $T = 5$ °K. When the temperature was increased to 23.4 °K and the intensity of the magnetic peaks was decreased by more than a factor of 8, the two peaks still had the same intensity ratio to better than 2%; therefore, extinction was assumed to be absent.

The correction for critical magnetic scattering is somewhat more difficult. This scattering has Lorentzian line shape and is strongly temperature dependent, diverging at T_N and decreasing rapidly both above and below T_N . However, by utilizing the distinctive line shape of the Bragg scattering, it was possible by successive approximation to estimate the additional Lorentzian component in the scattering at each temperature. This process was aided considerably by the fact that near T_N [see Fig. 1(c)] the tail of the Lorentzian was prominent. In any case, only the final two data points were appreciably affected so that these corrections played the role of a consistency check rather than actually altering the final values of D or β .

III. RESULTS

In the temperature interval 5–23.4 °K ($T_N = 23.553$ °K), the intensities of both the (1 0 $\bar{1}$) and the (2 0 1) reflections were measured. (See Figs. 1 and 2 of the previous paper for the crystal structure and the corresponding reciprocal lattice.) Both of these are purely magnetic peaks, so background consisted of double-Bragg- and incoherent-scattering contributions, which were small. At 23.4 °K ($M/M_0 = 0.35$), the intensity of the (2 0 1) reflection was only eight times the background and the accuracy was no longer sufficient to warrant higher-temperature measurements. On the other hand, at 23.525 °K ($M/M_0 = 0.21$), the (1 0 $\bar{1}$) reflection was still sufficiently intense to ensure reasonable accuracy. Below 23.475 °K no correction was made for the critical scattering; above, the effect was significant and the correction was made. In order to calculate the magnetization, integrated rather than peak intensities of the φ scans were used. We restricted ourselves to the region out to twice the full width at half-maximum, however, in order to keep the background from becoming important. Taking the integrated intensity reduced the statistical error and averaged the effects of not measuring at precisely repeatable points on the peak.

As the intensity of the magnetic peak decreased, the counting time was increased in order to minimize the *statistical* error, relative to the various other uncertainties. The critical scattering was assumed to be accurate to only $\pm 20\%$. Table I gives the intensity and the critical-scattering correction at each temperature. In order to compute

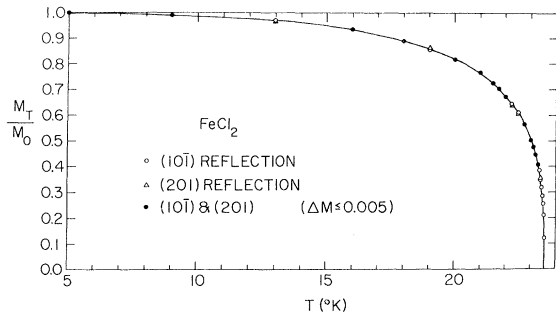


FIG. 2. Reduced sublattice magnetization in FeCl_2 as a function of temperature. A single filled dot is shown when the difference between the values of M_T/M_0 deduced from the $(1, 0, \bar{1})$ and $(2, 0, 1)$ reflections is less than 0.005.

the relative magnetization $[M_T \propto (I_T)^{1/2}]$, it was assumed that the magnetization at 5 °K was the saturation value. Taking $M_{5^\circ\text{K}} = M_0$, then at each temperature $M_T/M_0 = (I_T/I_{5^\circ\text{K}})^{1/2}$, and this quantity is plotted in Fig. 2. Only at 23.525 and 23.55 °K was there a significant uncertainty associated with the estimation of background and critical scattering for the $(1\ 0\ \bar{1})$ peak. At most other points the uncertainty in temperature was the largest source of error.

IV. ANALYSIS

The magnetization was fitted to the power law [Eq. (1)] by the method of least squares. In determining the appropriate weighting factors for the $(1\ 0\ \bar{1})$ reflection the magnetization at 23.55 °K was assumed to be known to no better than $\pm 2\%$, at 23.525 and 23.50 to $\pm 1\%$, and at all other temperatures to $\pm \frac{1}{2}\%$. In addition, temperatures below 21.5 °K were not included in the final fit, because when they were included the quality of the fit decreased appreciably. This simply reflects the breakdown of the power law [Eq. (1)] away from T_N . Above 21.5 °K any point could be removed without affecting either the quality or the results of the fit.

The result for the best fit shown in Fig. 3, with all parameters allowed to vary freely, is

$$\begin{aligned} \beta &= 0.286 \pm 0.003, \quad T_N = 23.553 \pm 0.002 \text{ °K}, \\ D &= 1.469 \pm 0.003, \end{aligned} \quad (3)$$

where the error bars are one-standard-deviation statistical errors. Taking into account possible systematic errors together with the uncertainties in the temperature measurement, we believe that more realistic values with errors are

$$\begin{aligned} \beta &= 0.29 \pm 0.01, \quad T_N = 23.553 \pm 0.01 \text{ °K}, \\ D &= 1.47 \pm 0.02. \end{aligned} \quad (4)$$

The value of T_N is well within the limits established

by others,^{9,10} but as discussed previously it is not considered as an absolute value, because of the possible existence of a temperature gradient between the sample and the thermometer. The value of D depends, of course, on the assumption that $M_{5^\circ\text{K}} = M_0$. Other measurements^{1,11} report a temperature-independent magnetization from 2 to 6 °K so that $M_{5^\circ\text{K}}$ most certainly differs from its 0 °K value by much less than the quoted error in D . The results for D and β are both satisfyingly close to the theoretical values and serve to verify that the Ising model for FeCl_2 is a good description.

The value we find for β , 0.29 ± 0.01 , does, of course, differ from the theoretical rigid-lattice Ising value of 0.313 ± 0.003 by an amount greater than the quoted errors. However, we do not believe that this apparent discrepancy should be overinterpreted. Indeed, in at least three other Ising systems [dysprosium aluminum garnet (DAG),¹² β brass,¹³ CoO ¹⁴] the bare values for β (0.26 ± 0.02 , 0.305 ± 0.005 , 0.244 ± 0.015 , respectively) are consistently lower than the theoretical rigid-lattice value. In the latter two materials this difference has been explained on the basis of lattice effects. Given the complexity of the magnetism in FeCl_2 and the fact that the spins are strongly coupled to the lattice, it seems likely that such exponent-renormalization phenomena are playing a role here as well.¹⁵

It is of interest to compare these results for FeCl_2 more directly with theory and with other experimental systems. The value of D we obtain agrees to within experimental error with that deduced by Essam and Fisher¹⁶ for the body-centered-cubic (bcc) $S = \frac{1}{2}$ Ising model. We choose, therefore, to compare our results directly with this model; the results are shown in Fig. 4. From the figure it may be seen that the bcc $S = \frac{1}{2}$ Ising model gives a good description of the order parameter in FeCl_2 at all temperatures. There is a small systematic discrepancy at intermediate temperatures which originates in the slight differences in D , β for the two systems. Calculations have also been performed

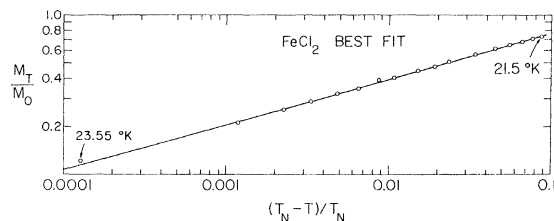


FIG. 3. Best fit of the reduced sublattice magnetization to the power law $M_T/M_0 = D(1 - T/T_N)^\beta$ with $D = 1.469$, $T_N = 23.553 \text{ °K}$, $\beta = 0.286$. Points below 21.5 °K deviate from the straight line, reflecting a breakdown of the power-law behavior.

by Fox, Guttman, and Gaunt⁶ for the simple-cubic $S=1$ Ising model. They find the values $D=1.43$, $\beta=0.313$, again similar to our results for FeCl_2 , albeit outside of the error limits. The consequent order-parameter curve is similar to that shown for the bcc $S=\frac{1}{2}$ Ising model although it lies slightly below the exhibited curve, thus enhancing the disagreement at intermediate temperatures. Nevertheless, the agreement in the critical region is sufficiently satisfactory that one would hope that tricritical-point series-expansion calculations for these models might be directly applicable to FeCl_2 . This represents an important simplification since the corresponding calculations for the true FeCl_2 structure and Hamiltonian would be extremely difficult.

In Fig. 4, the neutron-diffraction data of Norvell and Als-Nielsen¹³ on the order-disorder transition in β brass (CuZn) at 736 °K are also displayed. The temperature variations of the normalized order parameters in FeCl_2 and β brass are indistinguishable not only in the critical region but in fact at all temperatures. This is a remarkable result especially when one considers the extreme difference in the nature of the two systems; this universality is, of course, the essence of critical phenomena. It should be noted, however, that Chipman and Walker¹⁷ using x-ray techniques have obtained results for brass which differ significantly from both the neutron results and the Ising theory. We cannot resolve this discrepancy here.

Finally, it should be emphasized that the critical behavior in FeCl_2 is clearly three dimensional in

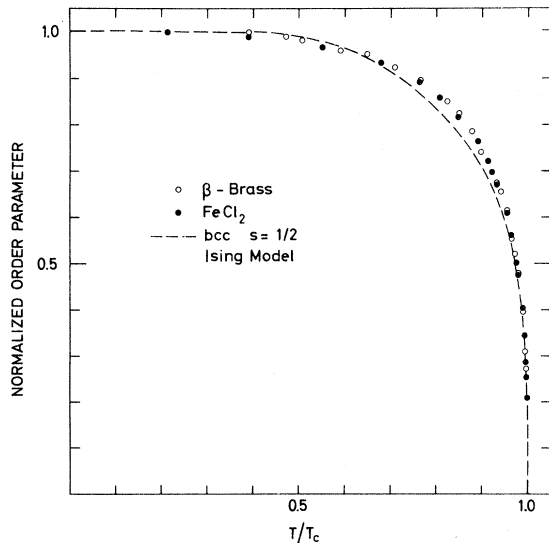


FIG. 4. Normalized order parameter vs reduced temperature in FeCl_2 , in β brass (Ref. 13) and in the bcc $S=\frac{1}{2}$ Ising model.

spite of the fact that the in-plane coupling is 20 times larger than the interplanar interaction. The three dimensionality of the critical behavior is even more clearly manifested in the wave-vector-dependent susceptibility which we discuss in Sec. V.

V. WAVE-VECTOR-DEPENDENT SUSCEPTIBILITY $T > T_N$

For a system of localized spins, with an interaction Hamiltonian of uniaxial symmetry, the neutron-scattering cross section in the quasielectric approximation is given by¹⁸

$$\frac{d\sigma^{\alpha\alpha}}{d\Omega}(\vec{Q}) = A(\vec{k}, \vec{k}') \frac{k_B T}{\mu_B^2} \sum_{\alpha} \frac{1}{g_{\alpha}^2} (1 - \hat{Q}_{\alpha}^2) \chi^{\alpha\alpha}(\vec{Q}), \quad (5)$$

where $A(\vec{k}, \vec{k}')$ is a constant and $\chi^{\alpha\alpha}(\vec{Q})$ is the wave-vector-dependent susceptibility. In the molecular-field model, for

$$|J^{zz}| > |J^{xx}| = |J^{yy}|,$$

the wave-vector-dependent susceptibility is given simply by

$$\chi^{\alpha\alpha}(\vec{Q}) = \frac{C/T_c}{(T - T_c)/T_c + [J^{zz}(\vec{\tau}) - J^{\alpha\alpha}(\vec{Q})]/J^{zz}(\vec{\tau})}, \quad (6)$$

where $J^{\alpha\alpha}(\vec{Q}) = \sum_{\vec{r}} e^{i\vec{Q}\cdot\vec{r}} J^{\alpha\alpha}(\vec{r})$ and $\vec{\tau}$ is a reciprocal-lattice vector. With $|J^{zz}| > |J^{xx}|$, $|J^{yy}|$, only $\chi^{zz}(\vec{\tau})$ diverges at T_c .

For $J_{zz}(\vec{\tau}) = 6J_1 - 6J_1'$, where J_1 and J_1' are the nearest-neighbor-intraplanar and interplanar ZZ exchange constants, respectively, it can be shown easily that

$$\chi^{zz}(Q_a^*0, 0) = A/(\kappa_a^{2*} + Q_a^{2*}) \quad (7)$$

and

$$\chi^{zz}(0, 0, Q_c^*) = A'/(\kappa_c^{2*} + Q_c^{2*}), \quad (8)$$

where

$$A' = -\frac{2}{3} (J_1/J_1') (6a/c)^2 A \quad (9)$$

and

$$\kappa_a^*/\kappa_c^* = (c/6a) (-\frac{3}{2} J_1'/J_1)^{1/2}. \quad (10)$$

In FeCl_2 , $\frac{1}{6}c = 5.81 \text{ \AA}$, $a = 3.58 \text{ \AA}$, and $J_1'/J_1 \approx -0.05$; therefore $\kappa_a^*/\kappa_c^* \approx 0.44$.

Thus, within the context of molecular-field theory, the critical scattering along both the a^* and c^* axes should have the form of simple Lorentzians with the full width at half-maximum (FWHM) of the former approximately one-half of that of the latter. Furthermore, only the Ising component, $\chi^{zz}(\vec{\tau})$, should be divergent at T_N .

It is interesting to note that the interplanar coupling is much more important for $\chi(\vec{Q})$ than for $\hbar\omega_{sw}(\vec{Q})$, the spin-wave energy. This is due to the fact that J_1' enters the former as $(-J_1'/J_1)^{1/2} \approx 0.2$, whereas it enters the latter as $(J_1'/J_1)^2 \approx 0.002$. Thus the susceptibility is predicted to be fully

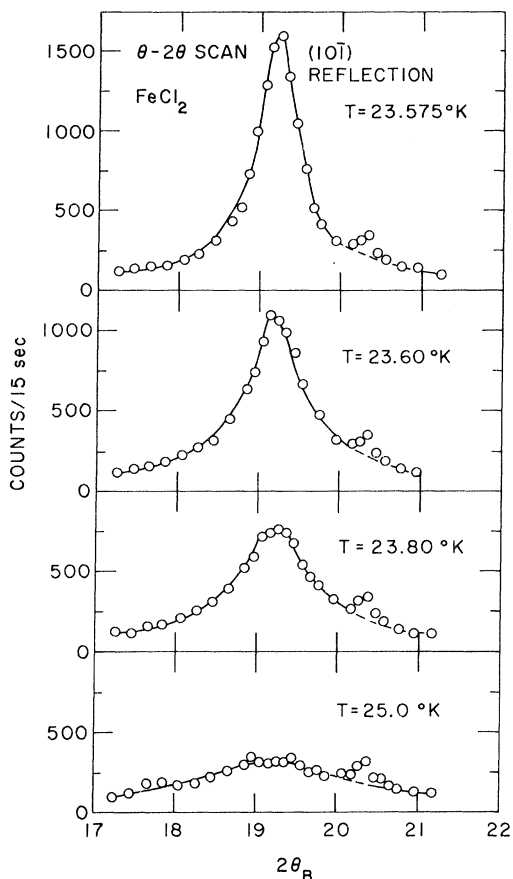


FIG. 5. Typical θ - 2θ critical-scattering scans above T_N at the $(1, 0, \bar{1})$ position. These correspond closely to scans along the a^* axis so that they measure the correlations within the ferromagnetic sheets. The small shoulder above $2\theta_B = 20^\circ$ originates in a satellite crystal.

three dimensional, whereas the spin waves simulate those of a two-dimensional ferromagnet.

We have carried out a qualitative survey of $\chi^{\alpha\alpha}(\vec{Q})$ above T_N . The experimental configuration was identical to that used for the sublattice magnetization measurements. More detailed quantitative work to determine the explicit critical exponents γ, ν characterizing, respectively, the staggered susceptibility $\chi^{\alpha\alpha}(\vec{r})$ and the correlation length $\xi = \kappa^{-1}$ was precluded by the large irregular mosaic of our sample. Scans were carried out mainly around the reciprocal-lattice points $(1, 0, \bar{1})$ and $(0, 0, 9)$. At these two reciprocal-lattice points one measures, respectively, the combinations $\chi^{\parallel} + \chi^{\perp}$ and $2\chi^{\perp}$, where the superscripts \parallel, \perp denote the components of $\chi^{\alpha\alpha}(\vec{Q})$ parallel and perpendicular to the c axis of the crystal. Typical experimental results are shown in Figs. 5 and 6. Figure 5 shows θ - 2θ scans at $(1, 0, \bar{1})$; these correspond to scans along the a^* axis. The data are found to approximate well to simple Lorentzians with a peak inten-

sity which increases drastically near T_N and a width which concomitantly approaches that of the instrumental resolution.

Additional scans at $T = 23.80^\circ\text{K}$ are shown in Fig. 6. From the figure it may be seen that the critical scattering observed around $(1, 0, \bar{1})$ arises almost entirely from χ^{\parallel} since the corresponding scan at $(0, 0, 9)$, which measures χ^{\perp} , is both flat and rather weak. We note also that the width of the Q_{c^*} scan is indeed somewhat larger than that of the corresponding Q_{a^*} scan as anticipated from molecular-field theory, although any explicit numerical comparison of κ_{c^*} and κ_{a^*} must await a proper deconvolution of data taken with a more perfect crystal. $\chi^{\parallel}(\vec{Q})$, thus, is fully three dimensional; this is to be contrasted with the critical scattering observed in the planar antiferromagnet K_2NiF_4 .¹ In that compound $\chi^{\parallel}(\vec{Q})$ is independent of Q_{c^*} so that the scattering has the form of a *ridge*; no such effect is observed here.

In summary, the critical scattering in FeCl_2 is found to correspond closely to that expected for a slightly aspherical three-dimensional Ising model. Detailed measurements of the critical exponents γ, ν would be of considerable interest. However, these necessitate higher-quality single crystals than

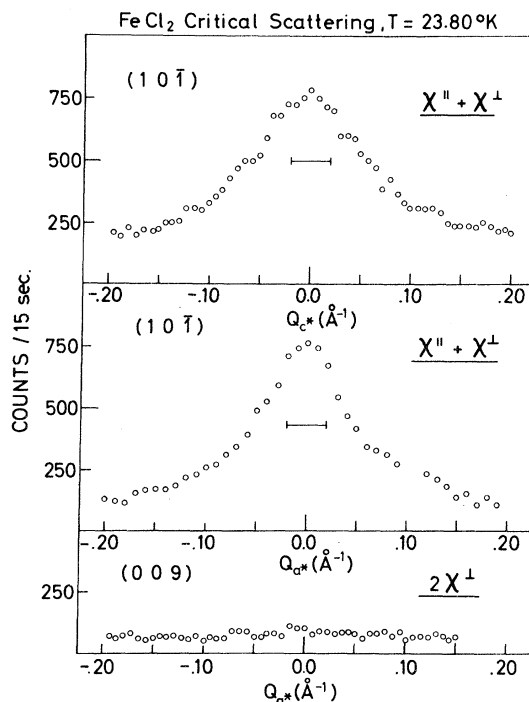


FIG. 6. Critical-scattering scans at 23.80°K along the a^* axis at $(0, 0, 9)$ and along the c^* and a^* axes at $(1, 0, \bar{1})$. The latter two scans measure the correlations between and within the ferromagnetic sheets, respectively. Q_{a^*} and Q_{c^*} are measured from the indicated reciprocal-lattice position.

those presently available to us.

VI. CONCLUSIONS

As stated in the Introduction and in the previous paper, this study was undertaken partially to examine the suitability of FeCl_2 for tricritical-point studies.¹⁹ The results are extremely encouraging. The sublattice magnetization is found to exhibit a simple power-law dependence on $(T_N - T)/T_N$ over more than two decades with an exponent $\beta = 0.29 \pm 0.01$. Existing theory predicts that β should change drastically near the tricritical point,^{3,20} probably to ~ 0.15 . The wave-vector-dependent susceptibility is found to exhibit critical behavior

which is both fully three dimensional and which is highly anisotropic. An Ising-model description, therefore, should be appropriate around the phase transition. We hope that this work will serve to stimulate theoretical work in the phase-transition properties of Ising antiferromagnets in a field.

ACKNOWLEDGMENTS

We should like to thank J. Als-Nielsen, M. Blume, G. Shirane, and W. P. Wolf for a number of helpful discussions on this work. One of us (R. J. B.) would like to thank the A. E. K. Risös for their hospitality during his part in writing this and the previous paper.

*Work at Brookhaven performed under the auspices of the U. S. Atomic Energy Commission.

[†]Guest scientist at Brookhaven National Laboratory, Upton, New York 11973.

¹R. J. Birgeneau, H. J. Guggenheim, and G. Shirane, *Phys. Rev. Letters* **22**, 720 (1969).

²For a general review on the theory of critical phenomena see M. E. Fisher, *Rept. Progr. Phys.* **30**, 615 (1967).

³I. S. Jacobs and P. E. Lawrence, *Phys. Rev.* **164**, 866 (1967); R. B. Griffiths, *Phys. Rev. Letters* **24**, 715 (1970).

⁴R. J. Birgeneau, W. B. Yelon, E. Cohen, and J. Makovsky, preceding paper, *Phys. Rev. B* **5**, 2607 (1972).

⁵D. Jasnow and M. Wortis, *Phys. Rev.* **176**, 739 (1968).

⁶A. J. Guttman, C. Domb, and P. F. Fox, *J. Phys. (Paris)* **32**, C1-354 (1971); P. F. Fox, A. J. Guttman, and D. S. Gaunt (unpublished).

⁷G. A. Baker, Jr., and D. S. Gaunt, *Phys. Rev.* **155**, 545 (1967).

⁸J. W. Essam and M. E. Fisher, *J. Chem. Phys.* **38**, 802 (1967).

⁹J. W. Stout, *Progr. Appl. Chem.* **2**, 287 (1961).

¹⁰H. Bizette, C. Terrier, and B. Tsai, *Compt. Rend.* **243**, 895 (1956).

¹¹W. H. Jones and S. L. Segel, *Phys. Rev. Letters* **13**, 528 (1964).

¹²J. C. Norvell, W. P. Wolf, L. M. Corliss, J. M. Hastings, and R. Nathans, *Phys. Rev.* **186**, 557 (1969).

¹³J. Als-Nielsen and O. W. Dietrich, *Phys. Rev.* **153**, 717 (1967); J. C. Norvell and J. Als-Nielsen, *Phys. Rev. B* **2**, 277 (1970).

¹⁴M. D. Reichtin, S. C. Moss, and B. L. Averbach, *Phys. Rev. Letters* **24**, 1485 (1970).

¹⁵M. E. Fisher, *Phys. Rev.* **176**, 257 (1968).

¹⁶See Ref. 8. The actual curve shown in Fig. 4 was computed by Norvell and Als-Nielsen (Ref. 13).

¹⁷D. R. Chipman and C. B. Walker, *Phys. Rev. Letters* **26**, 233 (1971).

¹⁸For a review see W. Marshall and R. Lowde, *Rept. Progr. Phys.* **31**, 705 (1968).

¹⁹An alternate system of considerable interest is the Ising antiferromagnet dysprosium aluminum garnet studied extensively by Wolf and co-workers [for a list of references see D. P. Landau, B. E. Keen, B. Schneider, and W. P. Wolf, *Phys. Rev. B* **3**, 2310 (1971)]. Results on this system indicate that the thermodynamic behavior of metamagnetic antiferromagnets in a field is rather more complicated than existing theories predict. This, of course, increases the importance of performing such experiments in FeCl_2 .

²⁰J. F. Nagle and J. C. Bonner, *J. Chem. Phys.* **54**, 729 (1971).